

On Spiral Structures in Tilings

Jessa Camille Duero¹, Bernhard Klaassen²

¹*Institute of Mathematical Sciences and Physics,
University of the Philippines Los Baños, Philippines*
jcduero@up.edu.ph

²*Fraunhofer Research Institution IEG, Bochum, Germany*
bernhard.klaassen@scai.fraunhofer.de

Abstract. In this paper, the existence of spiral structure in certain types of tilings is investigated. Following a question posed by Branko Grünbaum, it is demonstrated that all Archimedean tilings can be partitioned in a spiral like manner thereby fulfilling a definition given in 2017 for this visual effect. Furthermore, to show that this is not possible for every arbitrary periodic tiling, non “spirable” examples are constructed in the sense of this definition. Lastly, an intuitive result for one-armed spirals is established: one-armed spirals and periodic tilings cannot coexist.

Key Words: tiling, spiral tiling, periodic, one-armed spiral

MSC 2020: 52C20

1 Introduction

Spiral tilings have been featured in nature [11, 12] as well as in the ancient arts [8]. However, these were only considered as mathematical objects when the Voderberg spiral (Figure 1) was discovered in 1936. There have been studies on spiral tilings since then but these works focus on the construction of tiles [3, 4, 9] rather than on the recognition of spiral structures in a given tiling. This is because no formal definition had been published and most authors relied on the spiral appearance of the tilings. Grünbaum and Shephard first made an attempt to define spiral tilings in [5] (see exercises of Section 9.5), but it is not general enough and disregards the psychological aspect of spiral tilings. A recently proposed definition [6] (with a refinement in [7]) attempts to provide precision and extends the work beyond monohedral tilings (although it lacks the shortness and elegance of the older definition). In this paper, our goal is to examine the existence of spiral structures in certain types of tilings using the recently formulated more general definition.

First, let us clarify some terms: A *tiling* \mathcal{T} of the plane is a countable family of sets, called *tiles*, that cover the plane without gaps or overlaps of non-zero area. If the intersection of

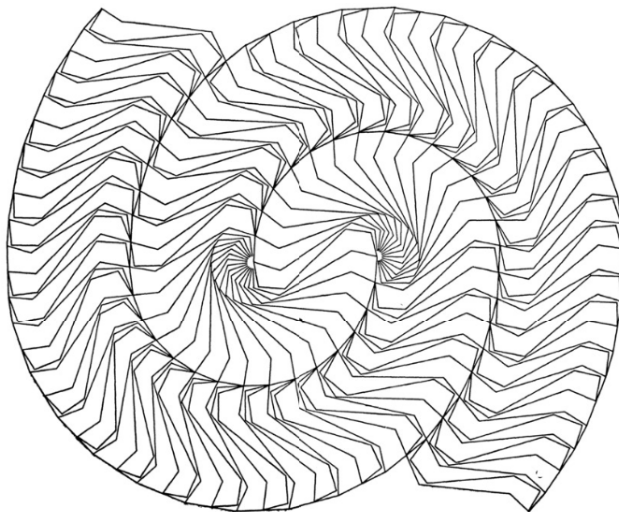


Figure 1: The Voderberg spiral [10].

three or more tiles is nonempty, then this intersection is called a *vertex* of \mathcal{T} . An *edge* is (part of) the intersection of two tiles that connects two vertices. In this research, all tiles considered are closed topological disks and uniformly bounded.

The isometries that map the tiling onto itself form the *symmetry group* of \mathcal{T} , denoted by $\mathcal{S}(\mathcal{T})$. If this group contains two linearly independent translations, \mathcal{T} is said to be *periodic*. All tilings considered in this paper are *k-hedral tilings*, that is, tilings that have only finitely many congruence classes with respect to the isometries present in each tiling's symmetry group. If a tiling has only one congruence class, it is called a *monohedral tiling* and a single representative of a congruence class is called a *prototile*.

Definition L ([6]). A partition of a plane tiling into more than one separate classes, called *arms*, is defined as a *spiral-like partition* or *L-partition* under the following conditions. (The plane is identified with the complex plane \mathbb{C} where the origin is represented by a selected point of the tiling.)

L1: For each arm A (as a union of tiles from one class) there exists a curve $\theta : \mathbb{R}_0^+ \rightarrow A \subset \mathbb{C}$ with $\theta(t) = r(t) \exp(i\varphi(t))$ called a *thread*, where both r and φ are continuous and unbounded and φ is monotone. Curve θ does not meet or cross itself or any thread from another arm of the tiling.

L2: For each tile T in A , the intersection of the interior of T with the image of θ is nonempty and connected.

A plane tiling, with uniformly bounded tiles, for which it is possible to create an L-partition is called *L-spirable* and an L-partitioned tiling is called an *L-tiling*.

In other words, for each spiral arm, a curve should enter the interior of each tile exactly once, winding infinitely around a central point without self-intersections.

Some examples of L-tilings are shown in the succeeding section. These L-tilings have no spiral structure and coloring the tiles is needed to distinguish the arms. Nevertheless, these can be partitioned in a manner in which they fulfill Definition L. Further definitions were given in [6] in order to differentiate such tilings from those with an inherent spiral structure. In the first part of this paper, we will focus on spiral-like tilings without requiring that these tilings be true spirals such as the Voderberg spiral. However, Definition L only caters multi-armed spiral tilings and thus, a separate definition is provided for one-armed spirals.

Definition O (for one-armed spirals). A k -hedral plane tiling without singular points is called a *spiral tiling with one arm* under the following conditions (The plane is identified with the complex plane \mathbb{C} where the origin is represented by a selected point of the tiling.):

- O1:** There exists a curve $b: \mathbb{R}_0^+ \rightarrow \mathbb{C}$ with $b(t) = r(t) \exp(i\varphi(t))$ called *spiral boundary*, where both r and φ are continuous and unbounded. Curve b does not meet or cross itself and runs completely on boundaries of tiles.
- O2:** If T_1, T_2 are direct neighbors and can be mapped (as a pair)¹ by rotation and translation onto another pair, these tiles must also be direct neighbors. This rule can be ignored if the image pair lies at the beginning of the boundary (i.e., contains $b(0)$). (*Direct neighbors* means here that $T_1 \cap T_2$ contains more than a finite number of points but not from the spiral boundary.)

2 L-spirability of Archimedean tilings

Archimedean tilings are vertex-transitive tilings that are made up of at most two regular polygonal tiles. A tiling with vertices surrounded by, in a cyclic order, n_1 -gon, n_2 -gon, \dots , and n_k -gon is denoted by $n_1.n_2 \dots n_k$. In [2], the authors demonstrated that all Laves tilings are L-spirable. In this section, we will show that their duals, the Archimedean tilings, are L-spirable as well.

The creation of L-partitions for this class of tilings is not as simple as in the Laves tilings. The simpler cases are listed in Figure 2. Threads are not shown in Figure 2 since their construction is straightforward. Among the Archimedean tilings, only the 3.12.12 tiling has complicated threads, as seen in Figure 3.

Note that a thread has the freedom to choose its path (the sequence of tiles it enters) in a spiral arm. In rare cases, it is necessary to run along the entire boundary of two tiles in order to avoid entering the interior of a tile twice. This is the case for the 3.12.12 tiling as shown in Figure 3. Thus, we have just demonstrated the following theorem:

Theorem 1. *All Archimedean tilings are L-spirable.*

Combining a result from [2] with the result established above gives us the following corollary:

Corollary 1. *All Archimedean tilings and their dual tilings are L-spirable.*

One might think that any well-behaved² tiling can be L-partitioned. In fact, in [2], the authors made a conjecture that every periodic monohedral tiling admits an L-partition, which is one of the open problems in [6]. However, we will demonstrate in the next section that this is not the case.

3 Counterexamples for L-spirability

The prototile shown in Figure 4a forms a periodic monohedral tiling \mathcal{T}_1 as seen in Figure 4b. \mathcal{T}_1 's symmetry group is $p4$, where the centers of four-fold symmetries are the centers of each tile and the vertices where four tiles meet. A fundamental domain for this tiling is any region

¹Here and below “mapped as a pair” means that the tiles can be respectively mapped by a direct isometry τ onto another pair of tiles $\tau(T_1)$ and $\tau(T_2)$.

²This term is used in [5] to describe tilings that are either normal, balanced or periodic.

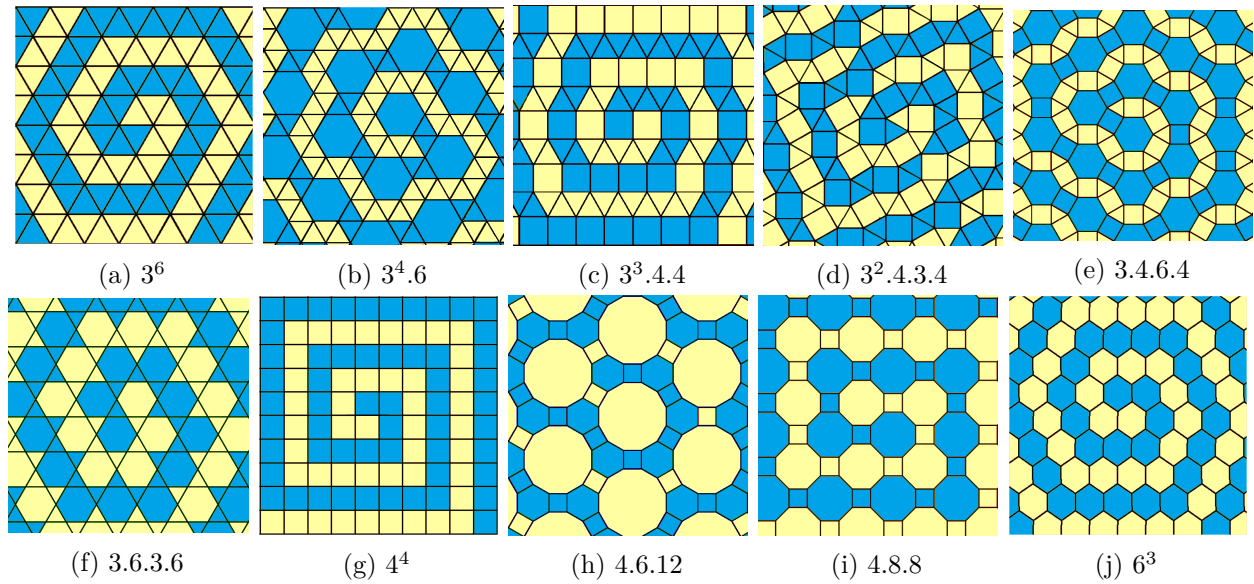


Figure 2: L-partitions of Archimedean tilings except the 3.12.12 tiling.

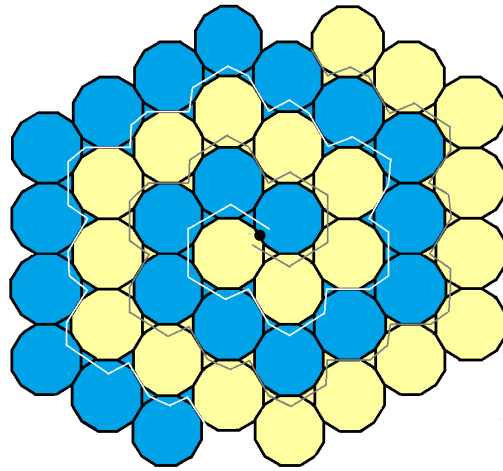


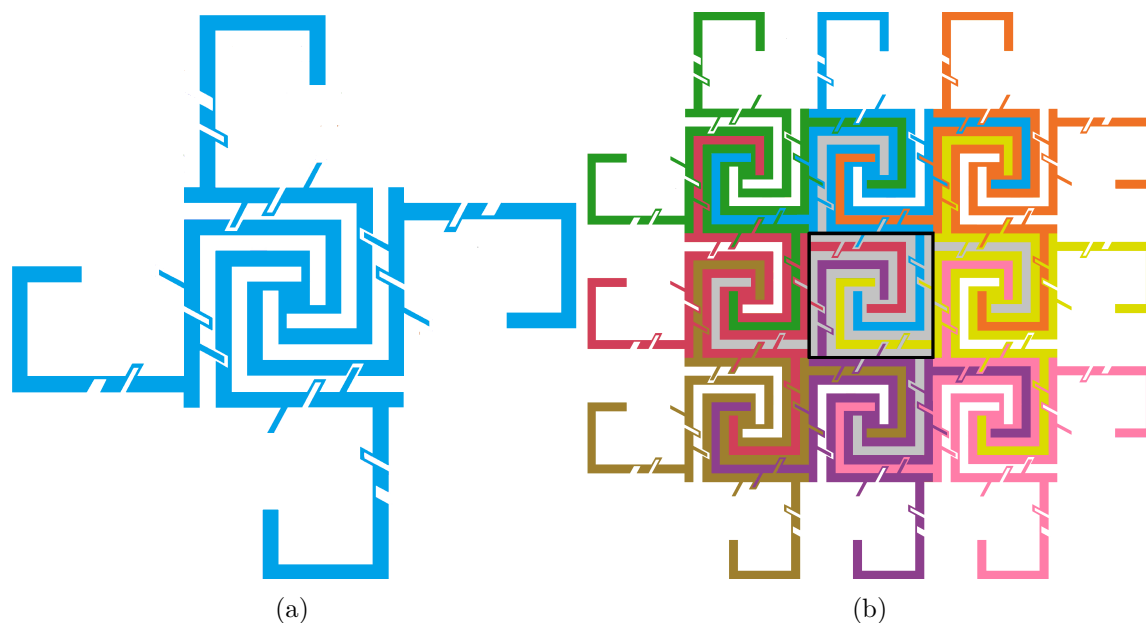
Figure 3: L-spirable Archimedean 3.12.12 tiling with threads sometimes running along tiles' boundaries.

that can be translated to cover the whole plane without overlapping. One possible choice of a fundamental domain of \mathcal{T}_1 is the area with a thicker border in Figure 4b, which we will denote by D_1 . The idea for constructing this prototile is from [1, Appendix A1 and Page 75], with some modifications for our purpose.

Let us consider a region on the east of the center of \mathcal{T}_1 . Suppose (without loss of generality) threads are running clockwise and a thread is passing through a region north of D_1 . Note that a thread cannot run entirely on the borders of D_1 , since otherwise, it will enter a tile twice. In particular, a thread running on one side of the square boundary of D_1 will enter the interior of the gray tile twice, which is forbidden by Definition L. With this, threads must cross the boundary of D_1 or its copies, and thus, it is enough to consider all threads crossing the upper edge of D_1 to illustrate that \mathcal{T}_1 is not L-spirable.

With these assumptions, we can identify all possible paths for a thread, each represented by the sequence in which the thread enters the tiles, as seen in Table 1.

There are sequences on Table 1 with tiles enclosed in a parenthesis. These entries

Figure 4: A non L-spirable periodic monohedral tiling \mathcal{T}_1

correspond to paths in which one includes the tile in parenthesis and another that does not. For instance, a thread that enters blue→gray→yellow runs a similar path with gray→yellow, except for the first tile in the sequence. Hence, we can simplify the table by writing the initial blue tile in the sequence in parenthesis. Figure 5 illustrates how a thread may enter these sequences of tiles. All of these paths violate the angular monotonicity of a thread with a center point assumed to lie at an appropriate distance westward of D_1 (indicated by an asterisk * in Table 1) or fail to maintain the connectedness of a thread within each tile (indicated by double asterisks **). For the unnumbered sequences in Table 1, we find that any possible thread arrives at a contradiction before reaching the sequence's last tile.

A thread may also enter D_1 from the northwest or northeast. However, threads will run along the same path as when you translate the tiling one tile to the right. For example, as a thread follows the path starting with the green tile outside D_1 and then entering D_1 through the gray tile, this is the same as a thread coming from the blue tile (outside D_1) and eventually entering the yellow tile (Column 3 of Table 1). Thus, we arrive at the same contradictions as the paths corresponding to threads 10–15 in Figure 5. Hence, the path of a thread entering D_1 from the northwest can be omitted in Table 1. Likewise, a thread entering D_1 from the northeast (orange→gray) is similar to the path starting from the blue tile and then entering the red tile (Column 1 of Table 1).

Finally, we must consider those threads that leave D_1 and later re-enter. The only paths through which a thread can re-enter D_1 are: (i.) crossing the western boundary of D_1 through the upper part of the red tile that extends into D_1 or through the part of the gray tile directly below the red part, or (ii.) crossing the eastern boundary through the gray tile. A re-entry into the lower half of D_1 can be omitted since no thread is able to reach this part. When a thread re-enters through the western boundary, such threads could be translated to the eastern edge of D_1 and thus are equivalent to threads leaving D_1 through the gray or yellow tiles (sequences that correspond to threads 10–15 in Figure 5). When a thread re-enters D_1 through the eastern boundary through the gray tile, this is equivalent to corresponding threads leaving through the western edge (threads 1–3). Threads crossing eastern or western edge

threads leaving D_1 through the western boundary	threads stopping within D_1	threads leaving D_1 through the eastern boundary
(gray→)red (1*) (gray→)red→green (2* and 3**)	gray→red (4** and 5*) gray (6* and 7**)	(blue→)gray→yellow (10* and 11**)
gray→red→brown gray→red→cyan	(gray→)blue (8*) blue→gray (9*) gray→yellow gray→violet	(blue→)gray→yellow→pink (12* and 13**)
		(blue→)gray (14*) yellow→gray (15**)
		(blue→)gray→yellow→dark gray

Table 1: Possible paths for a thread when it crosses the northern boundary of D_1

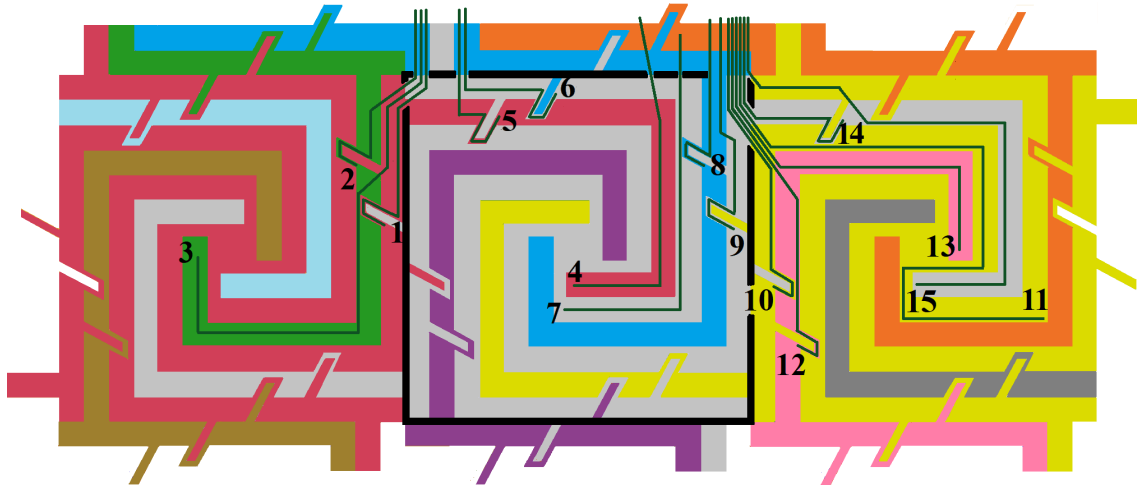


Figure 5: Some possible paths of threads as indicated in Table 1

more than twice are disregarded since an edge of D_1 lies within the union of only two tiles.

Although the sequences of tiles in Table 1 do not specify the exact behavior of threads in an L-tiling, it is guaranteed that any thread entering these sequences of tiles will yield the corresponding violation. For instance, two of the three paths for the sequence gray→red (1 and 5) contradict the inherent angular monotonicity of a thread. The other thread (4) cannot continue its path since otherwise it will enter the gray tile twice. Any thread that follows the gray→red sequence will always end up with one of the two contradictions indicated. Hence, \mathcal{T}_1 is unspirable in the sense of Definition L since it is impossible to have a thread that satisfies Conditions L1 and L2.

The nonconvexity of the prototile in the previous tiling plays a crucial role and one could conclude that such tiles are needed to construct non L-spirable tilings. The next tiling shows that this is not the case for 2-hedral tilings. Let us take a look at the periodic tiling \mathcal{T}_2 in Figure 6 which consists of convex tiles only. \mathcal{T}_2 has symmetry group pmm and its fundamental domain is made up of unit square tiles and rectangular tiles where the ratio of the square tiles to the rectangular tiles is 1:13.

Suppose \mathcal{T}_2 is L-spirable and let us consider a fundamental domain D_2 in \mathcal{T}_2 . Consider a thread θ of an arm in D_2 . Without loss of generality, let us assume the following: (i) the threads in \mathcal{T}_2 run clockwise, and (ii) the origin O of the complex plane is far enough southward of D_2 . Note that we can assume this without loss of generality because θ cannot change its direction since the rectangular tiles oriented horizontally in between the square tiles can

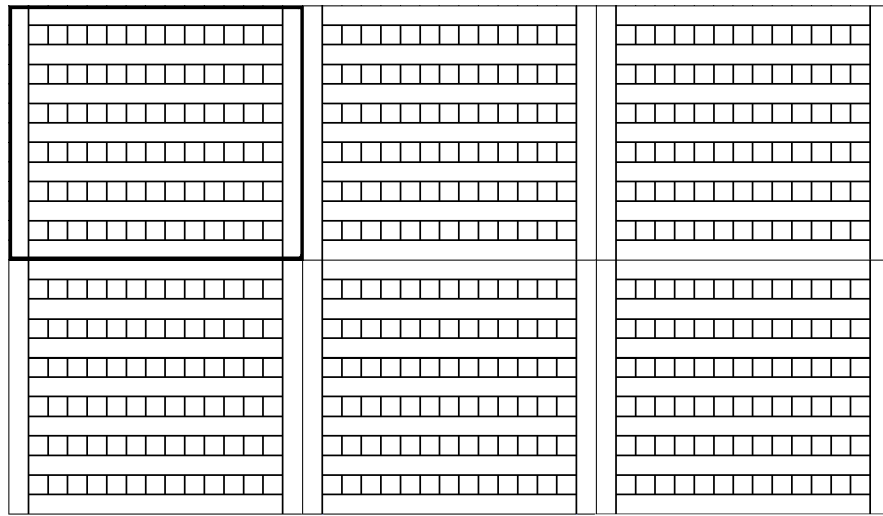


Figure 6: The periodic tiling \mathcal{T}_2 with its fundamental domain D_2 indicated by the thicker border

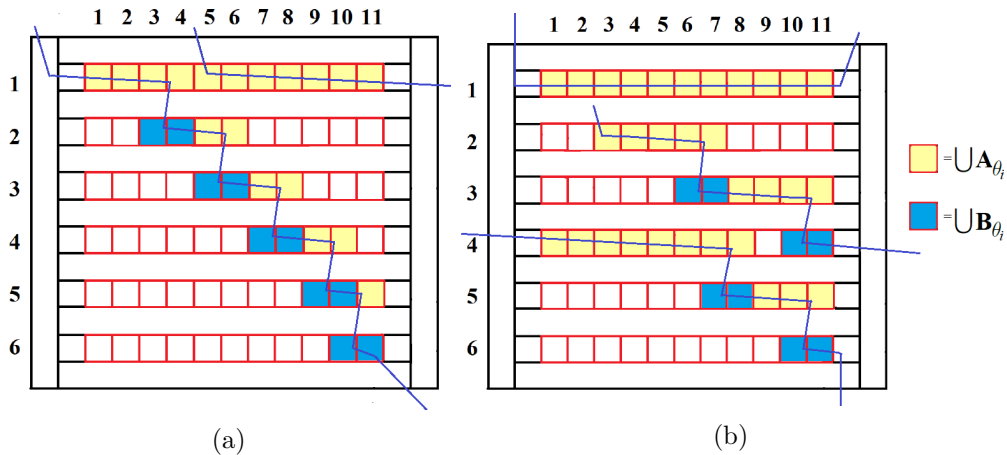


Figure 7: Possible paths for threads entering region R . Yellow and blue tiles make up $\cup A_{\theta_i}$ and $\cup B_{\theta_i}$, respectively.

only be crossed once. Now, thread θ passes through a sequence of red framed square tiles in Figure 7. Let R be the region consisting of the red framed square tiles. The tiles in R entered by θ can be partitioned into two sets, A_θ and B_θ , where A_θ contains the first red square tile that θ enters in each column and B_θ consists of all the other tiles in R entered by θ . Since R has 11 columns, $|A_\theta| \leq 11$. The number of tiles in B_θ may increase every time θ enters a new row.

Let $|B_\theta^n|$ be the number of elements in B_θ from row n . Provided that R lies far enough “northward” from O , to satisfy the monotonicity of θ , the angle of θ is limited such that no more than two tiles can lie in B_θ in every row. (This argument using a limited angle for the thread was also applied in a similar way to the first counter example.) Consequently, $|B_\theta^n| \leq 2$ holds for any row n .

Note that $|B_\theta^1| = 0$ and $|B_\theta^j| \leq 2$, $j = 2, 3, 4, 5, 6$. Thus, $|B_\theta| = \sum_{j=1}^6 |B_\theta^j| \leq (2)(5) = 10$. It follows that $|A_\theta| + |B_\theta| \leq 21$. The same holds for the other options in an analogous way: θ running upwards through R and θ running in anti-clockwise direction. At this point, we have shown that any thread intersecting region R will enter at most 21 red square tiles (with the origin far enough southward). Some possible paths for threads entering region R are

illustrated in Figure 7. Here, threads from one row of red squares enter the next row of red squares in a downward direction. However, these threads can also run in upward direction, yielding the same results for sets A_θ and B_θ . Now, each thread belongs to a spiral arm which each is a connected unbounded tile set. Since D_2 has four tiles on the boundary, there are at most four threads leaving region R .

Suppose there are four threads intersecting R . This means that all the boundary tiles belong to different arms. However, from the area of the red square tiles, the western boundary tile cannot be reached by a monotonous thread if the center is far enough southward. This implies that there are at most three threads intersecting R . This accounts only for at most 63 square tiles. Since there are 66 red square tiles, it is impossible to enter all the square tiles with three or fewer threads. Therefore, \mathcal{T}_2 is not an L-spirable tiling.

Theorem 2. *There exists a monohedral periodic tiling with a non-convex prototile for which no L-partition exists in the sense of Definition L. Furthermore, there exists a 2-hedral tiling with only convex tiles that is not L-spirable.*

The presented counterexamples even hold for L-tilings with infinitely many arms.

4 One-armed spirals

Unlike L-tilings, one-armed spirals cannot be induced by partitioning—the structure of the tiling itself can be viewed as a spiral with one arm.

In Definition O, the concept of direct neighbors in one-armed spirals is introduced. Here, the nonempty intersection of two tiles is an edge that does not lie on the spiral boundary b . The set containing all tile pairs sharing an edge in a k -hedral tiling can be partitioned into congruence classes such that every pair of tiles belongs to the same class as its image under a direct isometry. In particular, if T_i and T_j are two tiles in a tiling and $T_i \cap T_j$ is an edge, then all the images of T_i and T_j (as a pair) under rotation and translation belong to the same class as a pair. Such a class shall be called a *tile pair class*. Contrapositive from Definition O, if two tiles T_i and T_j do not contain $b(0)$ and $T_i \cap T_j$, which contains more than a finite number of points, lies on the spiral boundary, the rotational and translational images of $T_i \cap T_j$ should also lie on the spiral boundary. In particular, if the intersection of an element of a tile pair class that is disjoint from $b(0)$ lies on b , each pair in the class should also have an intersection that lies on b . Thus, we can associate a tile pair class to an edge class $[e]$ defined by the set of edges in a tiling whose elements are the images of e under direct isometries.

A sequence of edges $\{e_n\}$ can be created from the edges lying on the spiral boundary b whose order is determined by the function φ that gives rise to b . Consider an edge $e_k \in \{e_n\}$. If all edges in $[e_k]$ lie on b , then we call e_k a *strong b-edge*. If an element of $[e_k]$ belongs to a tile that contains $b(0)$, then it can be the case that not all elements of $[e_k]$ lie on b . We call $e_l \in \{e_n\}$ a *weak b-edge* if there exists e' in $[e_l]$ such that $e' \notin \{e_n\}$.

Suppose e_l is a weak b -edge. Then there exists e' in $[e_l]$ such that $e' \notin \{e_n\}$. This means that there are tiles T_1 and T_2 which are direct neighbors and $T_1 \cap T_2 = e'$. Note that e_l should be a part of a tile that contains $b(0)$, since otherwise, Condition O2 will not be satisfied. If all elements in the tile pair class of T_1 and T_2 are direct neighbors, except the tile pair that contains e_l , then e_l is the only edge in $[e_l]$ that lies on b . If there is a tile pair in the tile pair class of T_1 and T_2 that are not direct neighbors, say $\tau(T_1)$ and $\tau(T_2)$, then $\tau(T_1) \cap \tau(T_2)$ lies on b , and at least one of them contains $b(0)$. Since there are only finitely many tiles that may

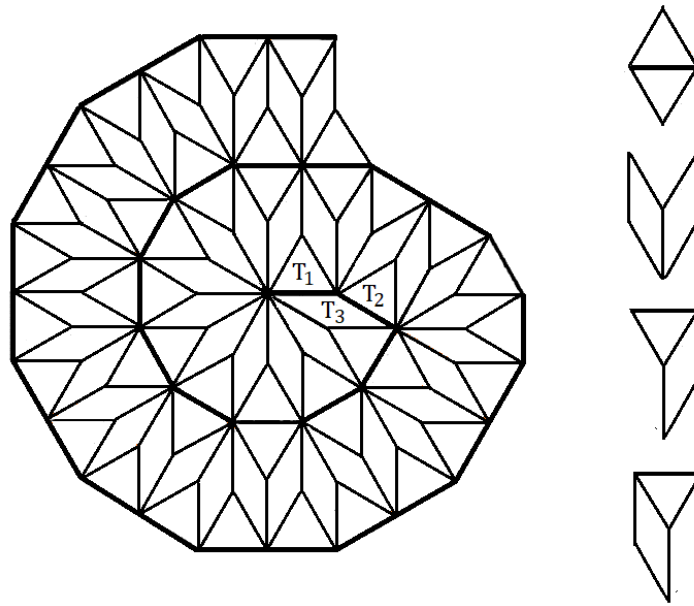


Figure 8: A one-armed spiral tiling with four tile pair classes.

contain $b(0)$, there are only finitely many images of $[T_1 \cap T_2]$ that lie on b . Thus, $[e_l] \cap \{e_n\}$ is finite.

In any case, we have shown that an edge class can only have finitely many weak b -edges. Since there are only a finite number of edges any tile can have and weak b -edges may only appear on tiles that have a nonempty intersection with $b(0)$, there are only finitely many classes that contain weak b -edges. Thus, we have the following lemma:

Lemma 1. *In an O-tiling there are only finitely many weak b -edges.*

In Figure 8, the thicker edges build the spiral boundary b . The first two edges in the sequence $\{e_n\}$ are $T_1 \cap T_3 = e_1$ and $T_2 \cap T_3 = e_2$. They are the only weak b -edges in this example since T_3 is the only rhombus with edges lying on the boundary.

Proposition 1. *A one-armed spiral tiling (according to Definition O) cannot be periodic.³*

Proof Idea. A subset of tiles near the starting point $b(0)$ can be distinguished from all other tiles that intersect with b . This contradicts the inherent repeating pattern of periodic tilings.

Proof. Assume a periodic O-tiling with spiral boundary b . The path of b along the edges creates a sequence of edges $\{e_n\}$ starting from $b(0)$. Let e_k be the first strong b -edge in this sequence. Note that there are only finitely many edges on b that are not strong b -edges by the lemma above. This guarantees the existence of e_k since the spiral boundary is an unbounded curve. Moreover, any edge aside from e_k sharing the first vertex of e_k (from $b(0)$) is either a weak b -edge or does not belong to b . Note that b cannot intersect the said vertex again since b is self-avoiding.

Since the tiling is assumed to be periodic, we can translate e_k , together with the tiles that have nonempty intersection with e_k , to a congruent region far enough away from $b(0)$. By definition of strong b -edge, the image of e_k , say $\tau(e_k)$, must be a strong b -edge, as well as both adjacent b -edges of $\tau(e_k)$, since weak b -edges can only exist near $b(0)$. This implies

³An analogue result for tilings containing an inherent multi-armed spiral structure was given in [2].

that the image region cannot be congruent to the pre-image region around e_k , which is a contradiction. \square

To give an example, consider the O-tiling in Figure 8 and the sequence of edges on its spiral boundary b starting from $b(0)$. In this tiling, the third edge in the said sequence is e_k . All the other edges after e_k are strong b -edges. As mentioned, the first edge on b that shares one vertex of e_k , i.e., $T_2 \cap T_3$, is a weak b -edge.

5 Conclusion

The motivation behind the definitions from [6] for spiral tilings is to capture, with mathematical rigor, the psychological effect alluded to by Grünbaum and Shephard in their 1987 work. The present work is a step towards answering Branko Grünbaum's question⁴ about general properties of tilings that may admit L-partitions, or fulfill other definitions from [6] (refined in [7]).

We have shown that there exists a periodic monohedral tiling that does not admit an L-partition, thereby answering one of the open problems in [6].

In our search for a complete characterization of L-spirable tilings, we have shown some interesting properties in this paper. For one-armed spiral tilings, we have proven an intuitive property: O-tilings cannot be periodic. We have also shown that all Archimedean tilings, which are 2-hedral periodic tilings, are indeed L-spirable. One can use the same method used in [2] to show that it is possible to construct an L-tiling for at least one example of each type of isogonal tiling using the same partitions constructed in Figure 2. Although nonconvexity played a crucial role in constructing our example for a non-spirable monohedral tiling, we have also presented a convex 2-hedral tiling that fails to admit L-partitions, demonstrating that convexity does not guarantee L-spirability.

References

- [1] C. ADAMS: *The Tiling Book An Introduction to the Mathematical Theory of Tilings*. American Mathematical Society, 2020.
- [2] J. DUERO, B. KLAASSEN, and R. SANTOS: *Spirals in Periodic Tilings*. Contributions to Discrete Mathematics **17**(1), 142–157, 2022. doi: 10.11575/cdm.v17i1.
- [3] M. GOLDBERG: *Central tessellations*. Scripta Math. **21**, 253–260, 1955.
- [4] B. GRÜNBAUM and G. SHEPHARD: *Spiral Tilings and Versatiles*. Mathematics Teaching **88**, 50–51, 1979.
- [5] B. GRÜNBAUM and G. SHEPHARD: *Tilings and Patterns*. W. H. Freeman and Company, 1987.
- [6] B. KLAASSEN: *How to Define a Spiral Tiling?* Mathematics Magazine **90**, 26–38, 2017.
- [7] B. KLAASSEN: *Is the spiral effect psychological?* Elemente der Mathematik **78**(1), 21–34, 2021. doi: 10.4171/em/465.

⁴Branko Grünbaum, private communication, 2016.

- [8] A. OVADIAH: *Geometric and Floral Patterns in Ancient Mosaics: A Study of their Origin in the Mosaics from the Classical Period to the Age of Augustus*. L'Erma di Bretschneider, Roma, 1980.
- [9] D. STOCK and B. WICHMANN: *Odd Spiral Tilings*. *Mathematics Magazine* **73**(5), 339–346, 2000. doi: 10.1080/0025570X.2000.11996873.
- [10] H. VODERBERG: *Zur Zerlegung der Umgebung eines ebenen Bereiches in kongruente*. *Jahresbericht der Deutschen Mathematikervereinigung* **46**, 229–231, 1936.
- [11] Y. YAMAGISHI and T. SUSHIDA: *Spiral disk packings*. *Physica D* **345**, 2016. doi: 10.1016/j.physd.2016.12.003.
- [12] Y. YAMAGISHI and T. SUSHIDA: *Archimedean Voronoi spiral tilings*. *Journal of Physics A: Mathematical and Theoretical* **51**(4), 2017. doi: 10.1088/1751-8121/aa9ada.

Received June 9, 2023; final form September 21, 2023.